Zylstra, E.R., Steidl, R.J., 2020. A Bayesian state-space model for seasonal growth of terrestrial vertebrates. Ecological Modelling.

Appendix A: Derivation of a seasonal model of growth

This derivation of a von Bertalanffy model of growth that allows for seasonal oscillations is based primarily on the work of Pitcher and Macdonald (1973) and Somers (1988).

We start by assuming that under constant temperature (or some other environmental factor that varies seasonally), rate of growth is proportional to the difference between length, L, and expected asymptotic length, L_∞:

$$\frac{\partial L}{\partial t} = G_1(L_\infty - L). \tag{A.1}$$

We note that G_1 is often replaced with K in traditional von Bertalanffy models, with K representing the growth rate coefficient or exponential rate of approach to asymptotic size (with units yr^{-1}) (Schnute and Fournier 1980). We also assume that for a given length, the rate of growth is proportional to ambient temperature:

$$\frac{\partial L}{\partial t} = G_2(T^\circ - T_m^\circ), \tag{A.2}$$

where T° represents ambient temperature and T_m° represents a critical minimum temperature at which the rate of growth equals zero. We further assume that ambient temperature varies seasonally, following a sinusoidal pattern over the course of a year such that:

$$T^\circ = A\cos\{2\pi(t - t_s)\} + B, \tag{A.3}$$

where A is the amplitude of the sinusoidal wave such that $2A$ is the difference between expected maximum and minimum temperature in a given year, B represents mean annual temperature, t is time (in years), and t_s is the time (in fractions of a year after 1 January) when growth is maximized. It follows that:

$$(T^\circ - T_m^\circ) = A\cos\{2\pi(t - t_s)\} + B - T_m^\circ. \tag{A.4}$$

If we assume $G_2(T^\circ - T_m^\circ) = H_2$, which is constant for a given temperature, we can combine equations 1 and 4 to obtain:

$$\begin{aligned}
\frac{\partial L}{\partial t} &= G_1(L_\infty - L) \\
\frac{\partial L}{\partial t} &= G_1\frac{H_2}{H_2}(L_\infty - L) \\
\frac{\partial L}{\partial t} &= \frac{G_1G_2}{H_2}(T^\circ - T_m^\circ)(L_\infty - L) \\
\frac{\partial L}{\partial t} &= \frac{G_1G_2}{H_2}(A\cos\{2\pi(t - t_s)\} + B - T_m^\circ)(L_\infty - L).
\end{aligned} \tag{A.5}$$

Therefore,

$$\frac{\partial L}{\partial t} = \frac{G_1G_2}{H_2}(B - T_m^\circ)\left(\frac{A}{B - T_m^\circ}\cos\{2\pi(t - t_s)\} + \frac{B - T_m^\circ}{B - T_m^\circ}\right)(L_\infty - L). \tag{A.6}$$

Now, if we let

$$k = \frac{G_1G_2}{H_2}(B - T_m^\circ) = \frac{G_1G_2(B - T_m^\circ)}{G_2(T^\circ - T_m^\circ)} = G_1\left(\frac{B - T_m^\circ}{T^\circ - T_m^\circ}\right) \tag{A.7}$$

and

$$C = \frac{A}{B - T_m^\circ}, \tag{A.8}$$

then

$$\frac{\partial L}{\partial t} = k(L_\infty - L)(C\cos\{2\pi(t-t_s)\}+1). \tag{A.9}$$

After integrating and consolidating constants of integration, we have:

$$log(L_\infty - L_t) = \frac{-kC}{2\pi}\sin\{2\pi(t-t_s)\} - kt + c. \tag{A.10}$$

We can then exponentiate and rearrange:

$$\begin{aligned} L_\infty - L_t &= e^{-\left(\frac{kC}{2\pi}\sin\{2\pi(t-t_s)\}+kt+c\right)} \\ L_t &= L_\infty - e^{-\left(\frac{kC}{2\pi}\sin\{2\pi(t-t_s)\}+kt+c\right)} \\ L_t &= L_\infty - e^{-\left(\frac{kC}{2\pi}\sin\{2\pi(t-t_s)\}+kt\right)}e^{-c}, \end{aligned} \tag{A.11}$$

and solve for e^{-c} by setting $t = t_0$ and $L_t = 0$:

$$\begin{aligned} 0 &= L_\infty - e^{-\left(\frac{kC}{2\pi}\sin\{2\pi(t_0-t_s)\}+kt_0\right)}e^{-c} \\ e^{-c} &= L_\infty e^{\left(\frac{kC}{2\pi}\sin\{2\pi(t_0-t_s)\}+kt_0\right)}. \end{aligned} \tag{A.12}$$

Replacing e^{-c} in equation 11 gives us:

$$L_t = L_\infty - e^{-\left(\frac{kC}{2\pi}\sin\{2\pi(t-t_s)\}+kt\right)}L_\infty e^{\left(\frac{kC}{2\pi}\sin\{2\pi(t_0-t_s)\}+kt_0\right)} \tag{A.13}$$

Now, if we let $S(t) = \frac{kC}{2\pi}\sin\{2\pi(t-t_s)\}$, then

$$\begin{aligned} L_t &= L_\infty\left(1 - e^{-\{S(t)+kt-S(t_0)-kt_0\}}\right) \\ L_t &= L_\infty\left(1 - e^{-\{k(t-t_0)+S(t)-S(t_0)\}}\right). \end{aligned} \tag{A.14}$$

Extending this to a capture-recapture model, we specify length at time $t+d$, where d is the time elapsed (in years) between captures:

$$L_{t+d} = L_\infty\left(1 - e^{-\{k(t+d-t_0)+S(t+d)-S(t_0)\}}\right). \tag{A.15}$$

Substituting $S(t+d) = S(t+d) + S(t) - S(t)$, we have

$$L_{t+d} = L_\infty - L_\infty\left(e^{-\{k(t-t_0)+S(t)-S(t_0)\}}\right)\left(e^{-\{kd+S(t+d)-S(t)\}}\right). \tag{A.16}$$

From equation 14, we know

$$\begin{aligned} L_\infty - L_t &= L_\infty - L_\infty\left(1 - e^{-\{k(t-t_0)+S(t)-S(t_0)\}}\right) \\ L_\infty - L_t &= L_\infty e^{-\{k(t-t_0)+S(t)-S(t_0)\}}, \end{aligned} \tag{A.17}$$

and substituting this into equation 16, we have

$$L_{t+d} = L_\infty - (L_\infty - L_t)e^{-\{kd+S(t+d)-S(t)\}} \tag{A.18}$$

$$\begin{aligned} L_{t+d} - L_t &= L_\infty - (L_\infty - L_t)\left(e^{-\{kd+S(t+d)-S(t)\}}\right) - L_t \\ L_{t+d} - L_t &= (L_\infty - L_t)\left(1 - e^{-\{kd+S(t+d)-S(t)\}}\right) \\ L_{t+d} &= L_t + (L_\infty - L_t)\left(1 - e^{-\{kd+S(t+d)-S(t)\}}\right). \end{aligned} \tag{A.19}$$

Note that t_0 and $S(t_0)$ have dropped out of the capture-recapture model. We need to provide auxiliary information about t_0 to estimate age (see Frazer et al. 1990). For canyon treefrogs, we can solve for t_0 in

equation 13 by assuming $L_t = 22.5$ when $t = 0$ (i.e., metamorphosis) (Wylie 1981). We further note that if $C = 0$ and t is the time at first capture, then equation 19 reduces to the non-seasonal "length at first capture" (LFC) model in Schofield et al. (2013).

Proof that a seasonal model of growth based on capture-recapture data is strictly non-decreasing

We want to show that $L_{t+d} = L_t + (L_\infty - L_t)\left(1 - e^{-\{kd+S(t+d)-S(t)\}}\right)$ is strictly non-decreasing for $C \in [0, 1]$. Assuming that t is time at first capture, and therefore constant for a given individual, we can show that L_{t+d} is strictly non-decreasing if the first derivative with respect to d is ≥ 0. Given that $L_\infty \geq L_t > 0$, this equates to showing that $f'(d) \geq 0$, where $f(d) = kd + S(t + d) - S(t)$.

$$\begin{aligned}
f'(d) &= \frac{\partial}{\partial d}[\, kd + S(t+d) - S(t)] \\
&= \frac{\partial}{\partial d}[\, kd] \, + \frac{\partial}{\partial d}\Big[\, \frac{kC}{2\pi} \sin\{2\pi(t + d - t_s)\}\Big] \\
&= k + \frac{kC}{2\pi}\frac{\partial}{\partial d}\Big[\, \sin\{2\pi(t + d - t_s)\}\Big] \\
&= k(1 + \frac{C}{2\pi} 2\pi \cos\{2\pi(t + d - t_s)\}) \\
&= k(1 + C\cos\{2\pi(t + d - t_s)\})
\end{aligned}$$

Because $C\cos\{2\pi(t + d - t_s)\} \in [-1, 1]$ for all $C \in [0, 1]$, $f'(d) \geq 0$ for all $k > 0$ and $C \in [0, 1]$. Therefore, L_{t+d} is strictly non-decreasing.

References

Frazer, N.B., Gibbons, J.W., Greene, J.L., 1990. Exploring Fabens' growth interval model with data on a long-lived vertebrate, *Trachemyts scripta* (Reptilia: Testudinata). Copeia 1990, 112–118.

Pitcher, T.J., Macdonald, P.D.M., 1973. Two models for seasonal growth in fishes. J. Appl. Ecol. 10, 599-606.

Schnute, J., Fournier, D., 1980. A new approach to length-frequency analysis: growth structure. Can. J. Fish. Aquat. Sci. 37, 1337-1351.

Schofield, M.R., Barker, R.J., Taylor, P., 2013. Modeling individual specific fish length from capture-recapture data using the von Bertalanffy growth curve. Biometrics 69, 1012-1021.

Somers, I.F., 1998. On a seasonally oscillating growth function. Fishbyte 6, 8-11.

Zylstra, E.R., Steidl, R.J., 2020. A Bayesian state-space model for seasonal growth of terrestrial vertebrates. Ecological Modelling.

Appendix B: Simulations to assess bias and precision of parameter estimates

Materials and methods

We used a series of simulations to evaluate the reliability of a seasonal model and to characterize bias in parameter estimates. Each simulated dataset comprised repeated length measurements for females only. We assumed captures occurred each month between March and October for two consecutive years (16 total occasions) and 40 new females were marked on each of the first 15 occasions, resulting in a total of 600 individuals. To ensure all individuals had ≥2 measurements in a given year, we assumed all individuals were recaptured during the survey immediately after they were marked; subsequently, we assumed an annual survival rate of 0.50 and constant recapture rate (p = 0.70 or 0.20).

To assess bias and precision of parameter estimates from our seasonal model of growth and determine whether it was necessary to model individual heterogeneity in asymptotic length, we simulated 200 datasets assuming seasonal variation in growth rates (C = 1, t_s = 0.6), individual heterogeneity in asymptotic length, L ($\bar{L}$ = 50, σ_β = 2) and length at first capture, λ ($\bar{\lambda}$ = 40, σ_α = 4), and no individual heterogeneity in growth rate (k = 3.0; Table B.1). We based simulated values on those we estimated for canyon treefrogs in 2014–2016. We assumed high recapture probabilities (p = 0.7) in the first 100 datasets, which resulted in an average of 3028 length measurements and 5.0 captures per individual; we assumed low recapture probabilities (p = 0.2) in the second 100 datasets, resulting in fewer length measurements (mean = 1719) and fewer captures per individual (mean = 2.9). For each dataset, we estimated growth parameters based on four models:

1) a seasonal model where we estimated C and estimated individual heterogeneity in L and λ;
2) a seasonal model where we fixed C = 1 and estimated individual heterogeneity in L and λ;
3) a seasonal model where we fixed C = 1 and estimated individual heterogeneity in λ but not L; and
4) a non-seasonal model where we estimated individual heterogeneity in L and λ.

To assess whether our model, which assumes no variation in growth rates among individuals, would provide reliable parameter estimates if there was individual heterogeneity in growth rates, we simulated 100 additional datasets where we assumed high recapture rates (p = 0.7), seasonal variation in growth rates (C = 1, t_s = 0.6) and individual heterogeneity in L ($\bar{L}$ = 50, σ_β = 2), λ ($\bar{\lambda}$ = 40, σ_α = 4), and k ($\bar{k}$ = 3.0, σ_γ = 0.2; Table B.2). We estimated growth parameters based on two models:

1) a seasonal model where we estimated C and estimated individual heterogeneity in L and λ but not k; and
2) a seasonal model where we fixed C = 1 and estimated individual heterogeneity in L and λ but not k.

Finally, to assess whether our model was robust to misspecification, we simulated 100 datasets where we assumed high recapture rates (p = 0.7), no seasonal variation in growth (C = 0), individual heterogeneity in L ($\bar{L}$ = 50, σ_β = 2) and λ ($\bar{\lambda}$ = 40, σ_α = 4), and no individual heterogeneity in k (k = 3.0; Table B.3). We estimated growth parameters based on a seasonal model where we estimated C and estimated individual heterogeneity in L and λ but not k.

For each estimating model, we used the same priors as those used in the analysis of the canyon treefrog data. For each simulated dataset and model used for estimation, we ran three Markov chains for 6000 iterations. After discarding the first 1000 iterations as adaptation and burn-in we retained 1 of every 5 iterations to summarize the posterior distribution. Gelman-Rubin statistics for all parameters were <1.1. For each parameter estimate, we calculated percent relative bias (PRB) by subtracting the true (simulated) value from the mean of the 100 marginal posterior means, dividing by the true value, and multiplying by 100. We also calculated credible interval coverage as the percentage of credible intervals that covered the true value.

Results

For the range of simulated values we explored, estimates of growth rate (k), mean asymptotic length ($\bar{L}$), standard deviation of individual asymptotic lengths (σ_β), and date of maximum growth (t_s) from a seasonal model that included individual heterogeneity in L were largely unbiased (Fig. 1; Table B.1). Measurement error (σ_y) was consistently overestimated, but only slightly (PRB = 3.5–4.4%). A model that assumed constant rates of growth performed poorly. Specifically, when growth rates fluctuated seasonally, a model that assumed constant growth overestimated both variance in asymptotic length and measurement error (PRB = 15-33%; Table B.1). Moreover, when individuals were born (or metamorphosed, if modeling post-larval growth in amphibians) when growth rates were at or near a seasonal maximum, a non-seasonal model overestimated the time required to reach sexual maturity by >4 weeks and underestimated the time required to reach 90% of asymptotic length by 13 weeks (Fig. 2).

Consistent with previous work (Wang, 2004; Zhang, Lessard, & Campbell, 2009), bias of parameter estimates in a seasonal model, particularly k and σ_y, increased greatly if models failed to account for individual heterogeneity in asymptotic length (Table B.1). In contrast, there was little gained by modeling individual heterogeneity in growth rates. Estimates of $\bar{k}$, $\bar{L}$, t_s, and σ_β, were unbiased, even when k varied by >5% among individuals (Table B.2).

Even when simulated growth rate was constant throughout a year, our seasonal model provided reliable estimates of $\bar{L}$ and k ($|\text{PRB}| \leq 0.25\%$; Table B.3). In these scenarios, posterior distributions of C were heavily skewed towards zero (mean = 0.03), indicating little evidence for seasonal fluctuations in growth rates, as expected.

References

Wang, Y.G., 2004. Estimation of growth parameters from multiple-recapture data. Biometrics 60, 670–675.

Zhang, Z., Lessard, J., Campbell, A., 2009. Use of Bayesian hierarchical models to estimate northern abalone, *Haliotis kamtschatkana*, growth parameters from tag-recapture data. Fish. Res. 95, 289–295.

Table B.1. Bias and precision of parameter estimates from four seasonal models of growth for 100 simulated datasets. Each dataset consisted of length measurements for 600 females with high (p = 0.7) or low (p = 0.2) recapture rates, assuming seasonal variation in growth and individual heterogeneity in asymptotic length ($\bar{L}$; $\sigma_\beta > 0$) but not growth rate (k). We present the mean of marginal posterior means, percent relative bias (PRB), and percent of credible intervals that contained the true value (Cov) for parameters in each of four models: 1) a seasonal model of growth that estimated variation in asymptotic length among individuals and estimated C, the magnitude of seasonal variation in growth; 2) a seasonal model of growth that estimated variation in asymptotic length among individuals and fixed C = 1; 3) a seasonal model of growth that assumed no variation in asymptotic length among individuals and fixed C = 1; and 4) a non-seasonal model of growth that estimated variation in asymptotic length among individuals. We did not calculate percent relative bias or credible interval coverage for C, when estimated, because the true value lies at the boundary of parameter space.

		Seasonal model, heterogeneity in L, estimated C			Seasonal model, heterogeneity in L, fixed C = 1			Seasonal model, no heterogeneity in L, fixed C = 1			Non-seasonal model, heterogeneity in L		
Parameter	Sim. value	Mean	PRB	Cov	Mean	PRB	Cov	Mean	PRB	Cov	Mean	PRB	Cov
p = 0.7													
$\bar{L}$	50.0	50.00	0.01	95	50.00	–0.01	94	50.29	0.58	32	49.78	–0.43	76
k	3.0	3.02	0.62	92	3.01	0.40	93	2.73	–9.05	16	3.88	29.34	0
C	1.0	0.97	--	--	--	--	--	--	--	--	--	--	--
t_s	0.6	0.60	–0.09	94	0.60	0.00	95	0.60	–1.00	84	--	--	--
σ_β	2.0	2.00	–0.23	92	1.99	–0.30	93	--	--	--	2.36	18.00	5
σ_y	1.2	1.24	3.48	50	1.24	3.47	50	1.81	50.73	0	1.52	26.99	0
p = 0.2													
$\bar{L}$	50.0	50.01	0.01	97	50.01	0.02	97	50.19	0.38	62	49.54	–0.91	42
k	3.0	3.02	0.54	93	3.00	0.00	94	2.84	–5.35	55	3.85	28.28	0
C	1.0	0.96	--	--	--	--	--	--	--	--	--	--	--
t_s	0.6	0.60	–0.09	96	0.60	0.00	97	0.60	0.00	98	--	--	--
σ_β	2.0	1.97	–1.68	94	1.97	–1.66	94	--	--	--	2.30	14.78	53
σ_y	1.2	1.25	4.37	59	1.25	4.32	60	1.66	38.24	0	1.60	33.14	0

Table B.2. Bias and precision of parameter estimates from two seasonal models of growth for 100 simulated datasets. Each dataset consisted of length measurements for 600 females with high (p = 0.7) recapture rates, assuming seasonal variation in growth, and individual heterogeneity in asymptotic length ($\bar{L}$; $\sigma_\beta > 0$) and growth rate ($\bar{k}$; $\sigma_\gamma > 0$). We present the mean, percent relative bias (PRB), and percent of credible intervals that contained the true value (Cov) for parameters in each of two models: 1) a seasonal model of growth that estimated variation in asymptotic length among individuals, assumed no individual variation in growth rates, and estimated C, the magnitude of seasonal variation in growth; and 2) a seasonal model of growth that estimated variation in asymptotic length among individuals, assumed no individual variation in growth rates, and fixed C = 1. We did not calculate percent relative bias or credible interval coverage for C, when estimated, because the true value lies at the boundary of parameter space.

		Heterogeneity in L, estimated C			Heterogeneity in L, fixed C = 1		
Parameter	Sim. value	Mean	PRB	Cov	Mean	PRB	Cov
$\bar{L}$	50.0	50.00	0.00	98	49.99	–0.02	98
$\bar{k}$	3.0	3.01	0.47	92	3.01	0.25	92
C	1.0	0.97	--	--	--	--	--
t_s	0.6	0.60	–0.08	92	0.60	0.00	93
σ_β	2.0	2.01	0.50	96	2.01	0.43	94
σ_γ	0.2	--	--	--	--	--	--
σ_y	1.2	1.24	3.47	40	1.24	3.49	40

Table B.3. Bias and precision of parameter estimates from a seasonal model of growth for 100 simulated datasets. Each dataset consisted of length measurements for 600 females with high (p = 0.7) recapture rates, assuming no seasonal variation in growth, individual heterogeneity in asymptotic length ($\bar{L}$; $\sigma_\beta > 0$), and no individual heterogeneity in growth rate (k; $\sigma_\gamma = 0$). We present the mean, percent relative bias (PRB), and percent of credible intervals that contained the true value (Cov) for parameters in a seasonal model of growth that estimated variation in asymptotic length among individuals, assumed no individual variation in growth rates, and estimated *C*, the magnitude of seasonal variation in growth. We did not calculate percent relative bias or credible interval coverage for *C* because the true value lies at the boundary of parameter space.

		Seasonal model with heterogeneity in *L*, estimated *C*		
Parameter	Sim. value	Mean	PRB	Cov
$\bar{L}$	50.0	50.02	0.03	96
k	3.0	3.01	0.24	96
C	0.0	0.03	--	--
σ_β	2.0	2.00	–0.25	96
σ_y	1.2	1.24	3.45	43

Zylstra, E.R., Steidl, R.J., 2020. A Bayesian state-space model for seasonal growth of terrestrial vertebrates. Ecological Modelling.

Appendix C: JAGS code for a seasonal, von Bertalanffy model of growth

Description of data needed to estimate seasonal growth

JAGS notation	Description
nind	Number of individuals
nmeas	Number of measurements, across all individuals
y	Vector (length = nmeas) of length measurements
ind	Vector (length = nmeas) of individual IDs associated with each measurement
t	Vector (length = nmeas) with time of first capture (in fractions of a year since 1 Jan) for individual associated with measurement
d	vector (length = nmeas) with time elapsed (in years) since first capture of individual associated with measurement
fem	Vector (length = nind) with 1 indicating the individual was a female, 0 if the individual was male, and NA if sex was unknown

Description of parameters in seasonal model

JAGS notation	Description (notation in the paper)
alpha[1]	Mean length at first capture, males (α_0)
alpha[2]	Difference between mean length at first capture in females and males (α_1)
beta[1]	Mean asymptotic length, males (β_0)
beta[2]	Difference between mean asymptotic length in females and males (β_1)
gamma[1]	Growth rate on the log scale, males (γ_0)
gamma[2]	Difference between growth rates (on the log scale) in females and males (γ_1)
C	Magnitude of seasonal oscillations in growth (C)
ts	Time of year when maximum growth occurs (t_s)
sd.meas	Measurement error (σ_y)
sd.alpha	Standard deviation of lengths at first capture (σ_α)
sd.beta[1]	Standard deviation of asymptotic lengths, males ($\sigma_{\beta(1)}$)
sd.beta[2]	Standard deviation of asymptotic lengths, females ($\sigma_{\beta(2)}$)
psi	Probability individual was female (ψ)

```
model {

for(m in 1:nmeas){
  y[m] ~ dnorm(mu[m],tau.meas)
  mu[m] <- lambda[ind[m]] + (L[ind[m]]- lambda[ind[m]])*
           (1-exp(-k[ind[m]]*d[m] -
            C*k[ind[m]]/(2*pi)*sin(2*pi*(t[m]+d[m]-ts)) +
            C*k[ind[m]]/(2*pi)*sin(2*pi*(t[m]-ts))))

  #for posterior predictive checks:
  y.pred[m] ~ dnorm(mu[m],tau.meas)
}

for(i in 1:nind){
  lambda[i] ~ dnorm(alpha[1] + alpha[2]*fem[i],tau.alpha)T(0,L[i])
  L[i] ~ dnorm(beta[1] + beta[2]*fem[i],tau.beta[fem[i]+1])T(0,)
  log(k[i]) <- gamma[1] + gamma[2]*fem[i]
  fem[i] ~ dbern(psi)
}

#Priors
alpha[1] ~ dnorm(0,0.001)
alpha[2] ~ dnorm(0,0.001)
beta[1] ~ dnorm(0,0.001)
beta[2] ~ dnorm(0,0.001)
gamma[1] ~ dnorm(0,0.001)
gamma[2] ~ dnorm(0,0.001)

tau.meas <- 1/(sd.meas*sd.meas)
sd.meas ~ dt(0,pow(5,-2),1)T(0,)

tau.alpha <- 1/(sd.alpha*sd.alpha)
sd.alpha ~ dt(0,pow(5,-2),1)T(0,)

for(i in 1:2){
  tau.beta[i] <- 1/(sd.beta[i]*sd.beta[i])
  sd.beta[i] ~ dt(0,pow(5,-2),1)T(0,)
}

psi ~ dunif(0,1)

pi <- 3.14159265359
C ~ dunif(0,1)
ts ~ dunif(0,1)

#Derived parameters:
L.fem <- beta[1] + beta[2]
lambda.fem <- alpha[1] + alpha[2]
k.male <- exp(gamma[1])
k.fem <- exp(gamma[1] + gamma[2])

}
```

Zylstra, E.R., Steidl, R.J., 2020. A Bayesian state-space model for seasonal growth of terrestrial vertebrates. Ecological Modelling.

Appendix D: Predicting length of canyon treefrogs based on seasonal and non-seasonal models

Materials and methods

We predicted lengths of post-metamorphic treefrogs over time based on a seasonal and non-seasonal model of growth. We compared the distributions of predicted lengths for three dates with the distribution of observed lengths for all individuals captured on or near those dates in 2015. Specifically, we predicted the mean length of 212 females and 212 males based on estimates of t_s and sex-specific estimates of k, $\bar{L}$, and σ_β from a seasonal form of the von Bertalanffy model (eq. 3; top panels in Figs. D.1–D.2). We assumed an equal number of males and females metamorphosed with an SVL of 22.5 mm on 1 July or 1 September. We also predicted the mean length of another 212 females and 212 males based on sex-specific estimates of k, $\bar{L}$, and σ_β from a non-seasonal form of the von Bertalanffy model (eq. 2; middle panels in Figs. D.1–D.2). For each sex and estimating model, we used Chi-squared tests to compare the distribution of predicted lengths on 15 April, 15 May, and 15 June with the distribution of observed lengths for all females or males captured in mid-April, mid-May, and mid-June, respectively. We included observed lengths for 50% of individuals captured with SVL < 40 (whose sex was unknown) during each capture occasion, assuming a 50:50 sex ratio.

Results

For females, the distribution of predicted lengths from the seasonal model more closely resembled the distribution of observed lengths in April and May than the distribution of predicted lengths from a non-seasonal model, which underestimated the frequency of smaller individuals (SVL < 44 mm). For males, the seasonal model underestimated the mean length of individuals in April and May, and the non-seasonal model overestimated the mean length of individuals in April and May compared to the observed distribution of lengths in 2015.

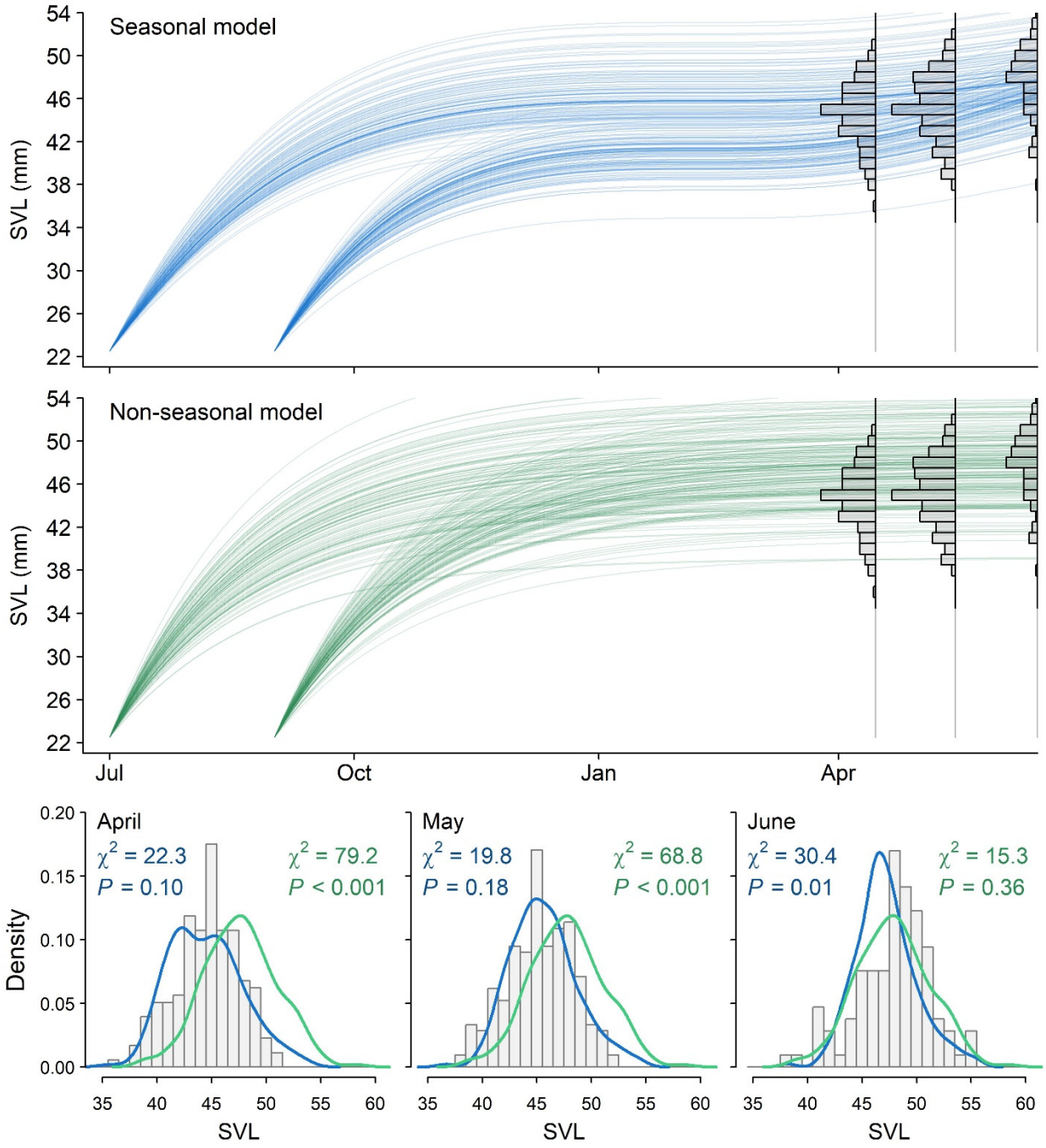

Figure D.1. Predicted growth of 212 females that metamorphosed with an SVL of 22.5 mm on either 1 July or 1 September. Predictions are from seasonal (top, blue) and non-seasonal (middle, green) forms of the von Bertalanffy model, where mean asymptotic length and growth rates differed between males and females and asymptotic length varied among individuals. Distribution of predicted lengths on 15 April, 15 May, and 15 June are compared with the distribution of observed lengths for all females captured in mid-April, mid-May, and mid-July, respectively (bottom). We include results of Chi-squared tests comparing predictions from a seasonal model with observed lengths (blue) and tests comparing predictions from a non-seasonal model with observed lengths (green).

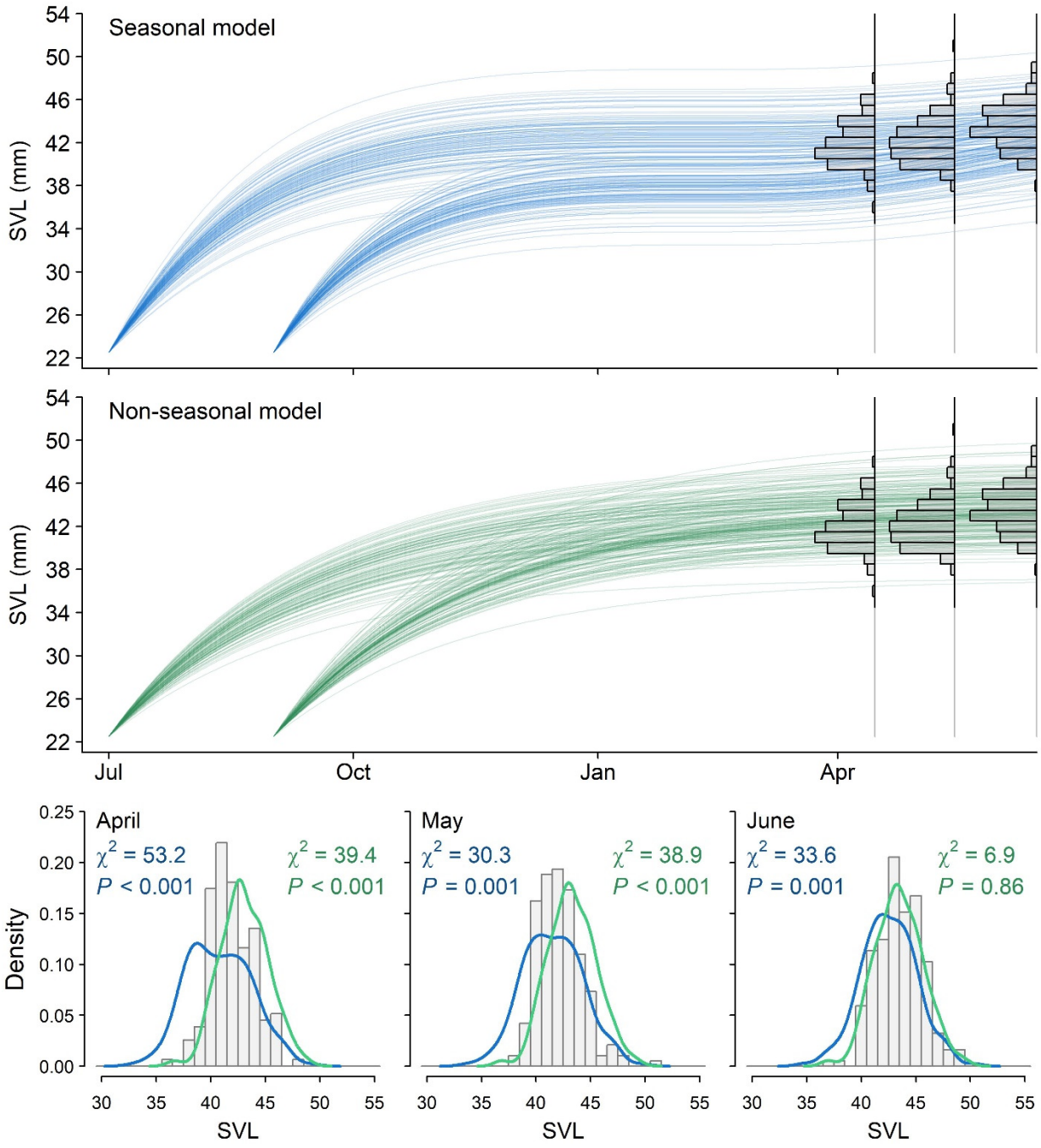

Figure D.2. Predicted growth of 212 males that metamorphosed with an SVL of 22.5 mm on either 1 July or 1 September. Predictions are from seasonal (top, blue) and non-seasonal (middle, green) forms of the von Bertalanffy model, where mean asymptotic length and growth rates differed between males and females and asymptotic length varied among individuals. Distribution of predicted lengths on 15 April, 15 May, and 15 June are compared with the distribution of observed lengths for all females captured in mid-April, mid-May, and mid-July, respectively (bottom). We include results of Chi-squared tests comparing predictions from a seasonal model with observed lengths (blue) and tests comparing predictions from a non-seasonal model with observed lengths (green).

Zylstra, E.R., Steidl, R.J., 2020. A Bayesian state-space model for seasonal growth of terrestrial vertebrates. Ecological Modelling.

Appendix E: Posterior predictive checks

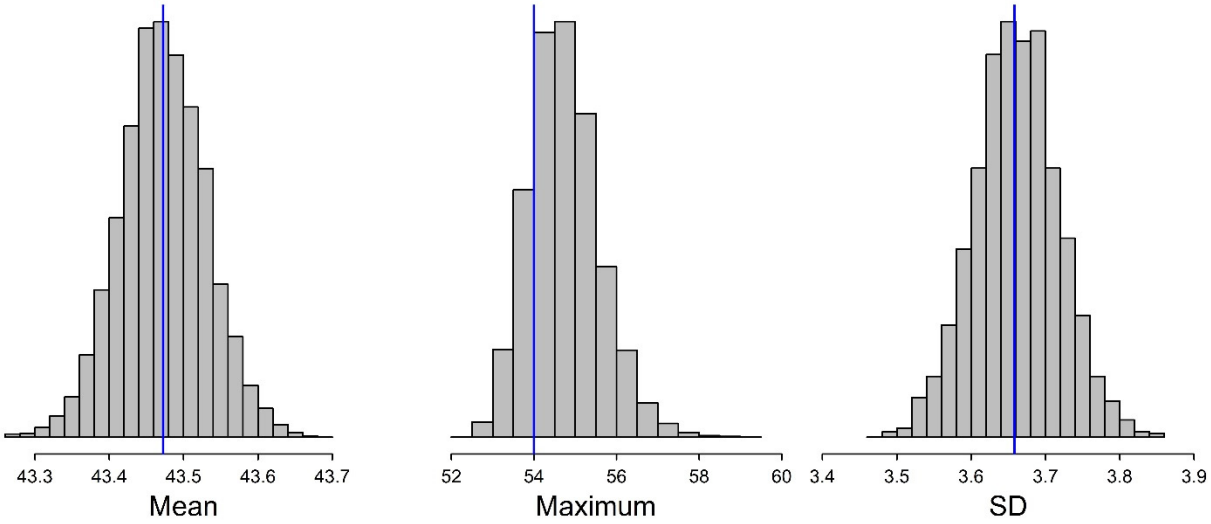

Figure E.1. Samples from posterior predictive distributions of the mean, maximum, and standard deviation (SD) of length measurements (mm), with observed values from measurements of 404 canyon treefrogs in blue.